Exclusive $(e,e'p)$ reaction at high missing momenta

V. Van der Sluys, J. Ryckebusch, and M. Waroquier
Institute for Theoretical Physics and Institute for Nuclear Physics, Proeftuinstraat 86, B-9000 Gent, Belgium
(Received 15 February 1996)

The reduced $(e,e'p)$ cross section is calculated for kinematics that probe high missing momenta. The final-state interaction is handled within a nonrelativistic many-body framework. One- and two-body nuclear currents are included. Electron distortion effects are treated in an exact distorted-wave calculation. It is shown that at high missing momenta the calculated $(e,e'p)$ cross sections exhibit a pronounced sensitivity to ground-state correlations of the random-phase approximation type and two-body currents. The role of these mechanisms is found to be relatively small at low missing momenta. [S0556-2813(96)00209-9]

PACS number(s): 25.30.Fj, 21.60.Jz, 24.10.Eq

I. INTRODUCTION

For a long time, the exclusive $(e,e'p)$ reaction for quasielastic (QE) kinematics has been considered as the ideal tool to study the single-particle properties of the nucleus [1–3]. One of the most remarkable conclusions drawn from the QE $(e,e'p)$ data was related to the low extracted spectroscopic factors that could not be explained within the independent-particle model (IPM). Long- and short-range correlations beyond the IPM are found to redistribute the hole strength over a range of excitation energies and to modify the nucleon momentum distribution with respect to the IPM prediction [4,5].

Recently, a renewed interest has been observed for the exclusive $(e,e'p)$ reaction. With the new generation of electron facilities the high-momentum components of the cross section have come into reach of experimental exploration. Initial results of this type of experiment are available for the ^{16}O$(e,e'p)$ [6] and ^{208}Pb$(e,e'p)$ [7] reactions. Data have been collected for proton knockout from the single-particle orbits near the Fermi level. The $(e,e'p)$ reaction at high missing momenta is expected to provide direct information on the nucleon momentum distribution at high momenta. As such the reaction could reveal information about the interaction of the nucleons at short internucleon distances. One should not forget, however, the following.

(a) Various studies [8–14] have shown that the single-particle spectral function gets strongly modified by short-range correlations (SRCs) at large excitation energies with only marginal effects at low energies. Accordingly, it is to be expected that short-range correlations hardly affect the exclusive $(e,e'p)$ knockout from the valence shells.

(b) The $(e,e'p)$ cross section is only directly related to the single-particle spectral function in the plane-wave impulse approximation (PWIA). The PWIA approach encompasses several assumptions. (i) The nuclear current operator is constrained to be a one-body operator. (ii) No final-state interaction (FSI) between the ejected nucleon and the residual nucleus is taken into account. (iii) Electron distortion effects are neglected. This assumption becomes questionable for heavy target nuclei.

It is clear that in order to extract reliable information on the nucleon spectral function from the $(e,e'p)$ reaction, the reaction mechanism has to be well understood. Our theoretical framework for the $(e,e'p)$ reaction goes beyond the PWIA and addresses the final-state interaction of the ejected nucleon with the residual core within a consistent many-body framework. We include one- and two-body photoabsorption mechanisms. In addition, the effect of Coulomb distortion on the electron wave functions is included exactly.

The outline of this paper is as follows. In Sec. II we briefly discuss the adopted $(e,e'p)$ formalism. Secs. III and IV deal with the results for the ^{16}O$(e,e'p)$ and ^{208}Pb$(e,e'p)$ reactions. Finally, some conclusions are drawn in Sec. V.

II. FORMALISM

In this paper we describe the scattering process of an electron with energy ϵ from a target nucleus, transferring an energy ω and momentum $\vec{q}$ to the nuclear system. The energy transfer ω is sufficient to eject a proton with momentum $\vec{p}_p$, energy E_p, and spin projection m_{s_p} out of the target nucleus.

In order to evaluate the $(e,e'p)$ cross section one has to calculate the nuclear response to the nuclear charge-current operator. In the one-photon exchange approximation and for constant $\vec{q}$-ω kinematics, the unpolarized cross section can be written in terms of longitudinal, transverse, longitudinal-transverse, and transverse-transverse parts:

$$\frac{d^6\sigma}{d\epsilon' d\Omega_e d\Omega_p dE_p} = \sigma_L + \sigma_T + \sigma_{LT} + \sigma_{TT}. \tag{1}$$

Each of these terms is related to the so-called nuclear structure functions, which in turn can be written as a specific combination of matrix elements between the initial and residual nuclear system of the charge-current four-vector $J_\mu(q)$ [15], i.e.,

$$\langle J_R M_R ; \vec{p}_p, 1/2 m_{s_p} | J_\mu(q) | J_i M_i \rangle, \tag{2}$$

where $|J_i M_i\rangle$ and $|J_R M_R\rangle$ describe the target and residual nucleus.

At this point the nuclear structure model and the photoabsorption mechanism need to be settled. The initial nuclear state and final-state interaction of the ejected proton with the residual nucleus is treated self-consistently in the many-body formalism as outlined in Ref. [16]. The final nuclear state is evaluated through a phase shift analysis based on a partial-wave expansion. The bound and continuum single-particle states are determined with the same potential, i.e., a Hartree-Fock (HF) potential generated with an effective interaction of the Skyrme type [17]. We go beyond the independent-particle model and incorporate long-range correlations not implemented in the HF approach. This is achieved in the random-phase approximation (RPA). The RPA states can be seen as a linear combination of one-particle–one-hole and one-hole–one-particle excited states out of a correlated ground state. The ground state of the target nucleus implicitly includes the long-range two-particle–two-hole correlations induced by the residual interaction.

For the photoabsorption mechanism, we assume that the virtual photon is absorbed on one or two nucleons in the nucleus. This means that the nuclear current has a one- and two-body part: $J_\mu(q)=J_\mu^{(1)}(q)+J_\mu^{(2)}(q)$. The transverse nucleonic one-body current consists of the well-known convection and magnetization current. The two-body current is taken from a nonrelativistic reduction of the lowest-order Feynman diagrams with one exchanged pion and intermediate Δ_{33} excitation. This procedure gives rise to the well-known ''seagull'' terms, the pion-in-flight term, and terms with a Δ_{33} excitation in the intermediate state [18,19]. In this nonrelativistic approach the nuclear charge operator is not affected by two-body contributions.

For heavy target nuclei, the model has to account for electron distortion effects. The distortions of the initial and the final electron due to the static Coulomb field generated by the protons in the nucleus are treated exactly in a Coulomb distorted-wave Born approximation calculation [20]. Details regarding the adopted numerical procedure are planned to be reported elsewhere [21]. When it comes to the treatment of electron distortions, our approach is very similar in nature to the one reported earlier by Jin *et al.* [22,23] and Udías *et al.* [24].

As is commonly done in the analysis of the quasielastic $(e,e'p)$ reaction, the calculations and the data are plotted as a reduced cross section that is derived from the cross section in the following way:

$$\rho_m(p_m,E_x)=\frac{1}{p_p E_p \sigma_{ep}}\left(\frac{d^6\sigma}{d\epsilon' d\Omega_e d\Omega_p dE_p}\right). \qquad (3)$$

Throughout this paper, we use the so-called CC1 off-shell electron-nucleon cross section $\sigma_{ep}=\sigma^{\mathrm{cc1}}$ as derived by De-Forest [25]. The missing momentum is defined according to $\vec{p}_m=\vec{p}_p-\vec{q}$. The sign convention for the missing momentum p_m is chosen such that p_m is negative for a proton ejected in the half plane determined by the initial electron momentum and bordered by the momentum transfer. For proton ejection in the other half plane, the missing momentum is considered to be positive. The excitation energy of the residual nucleus is denoted by E_x.

It should be stressed that only in the case that the FSI, two-body currents, and electron distortion can be neglected, the reduced cross section coincides with the single-particle spectral function and can be directly related to the microscopic predictions for this quantity. In a similar way, the missing momentum p_m can only be interpreted as the momentum of the nucleon before it was struck by the virtual photon in the PWIA. This means that a careful examination of the various higher-order effects needs to be performed before one can associate the high-p_m data with the high-momentum components of the spectral function. In this paper, the outlined formalism is applied to the exclusive $^{16}\mathrm{O}(e,e'p)$ and $^{208}\mathrm{Pb}(e,e'p)$ reactions.

III. RESULTS FOR $^{16}\mathrm{O}(e,e'p)$

The $^{16}\mathrm{O}(e,e'p)$ reaction has been studied for different electron kinematics. As outlined in the preceding section, our model implements two types of nucleon-nucleon correlations beyond the IPM: long-range RPA correlations and meson-exchange and isobaric contributions. By varying the momentum transfer q for a fixed ϵ and ω, we can investigate the q dependence of these additional components in the model.

In Fig. 1 we plot the reduced cross section for electro-induced one-proton knockout from the $1p_{3/2}$ shell in $^{16}\mathrm{O}$. Comparing the HF reduced cross section with the IPM momentum distribution, a striking feature is that the final-state interaction of the ejected proton with the residual nucleus generates a lot of strength at high p_m. Further, the HF reduced cross section has a smoother p_m dependence compared to the IPM momentum distribution. The long-range RPA correlations considerably modify the reduced cross section at high p_m and leave the low-momentum components of the reduced cross section almost unaffected. From Fig. 1 it is also clear that for high-momentum transfer q, RPA correlations have an effect on the reduced cross section for the complete missing momentum range.

The contribution of the two-body nuclear currents in the model is investigated in Fig. 2 and is found to exhibit a very similar behavior for the three considered kinematics. In order to explain this behavior we *first* examine the transverse part σ_T of the cross section in more detail as this quantity is expected to show the largest sensitivity to the two-body currents. Figure 3 clearly demonstrates that the contribution from two-body nuclear currents becomes less important with increasing momentum transfer. However, the high-momentum components of the reduced cross section are probed in the tail of the transverse cross section where the one-body current contribution becomes rather small. It can be easily shown that for a fixed value of the missing momentum p_m the proton scattering angle decreases with increasing q (marked with arrows in Fig. 3). Furthermore, in this scattering region, the two-body contribution to the cross section decreases with increasing scattering angle. This feature can be easily explained by the fact that for higher scattering angles (higher p_m) mainly high-momentum mesons are exchanged between the nucleons and the fact that the meson propagator decreases with increasing meson momentum. The previous considerations allow us to conclude that even small contributions from mesonic currents come into play when studying the high-momentum side of the $(e,e'p)$ cross sec-

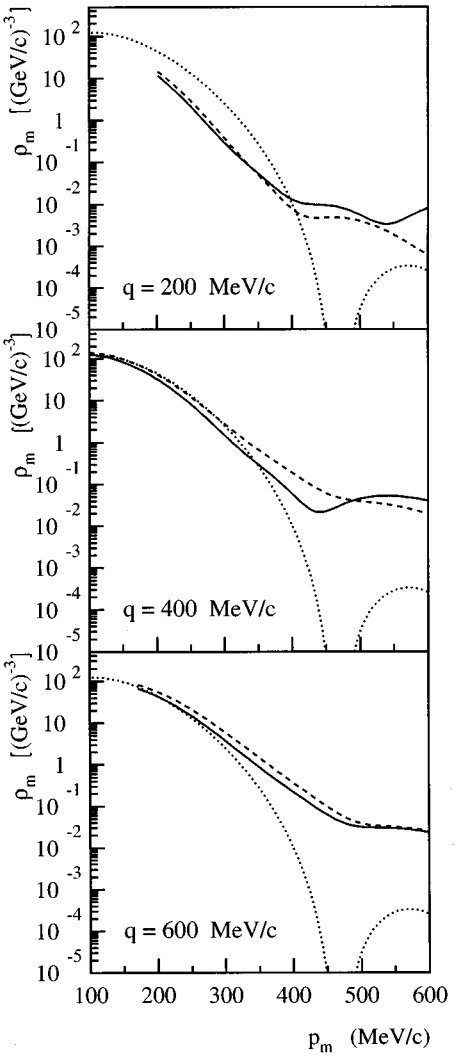

FIG. 1. Reduced cross section for proton knockout from the $1p_{3/2}$ shell in ^{16}O for $\epsilon = 500$ MeV, $\omega = 100$ MeV, and different values of the momentum transfer. The dotted line represents the IPM momentum distribution and the dashed line depicts the reduced cross section in the HF framework including only one-body components in the nuclear current. For the solid line long-range RPA correlations are accounted for. The curves are not multiplied by a spectroscopic factor.

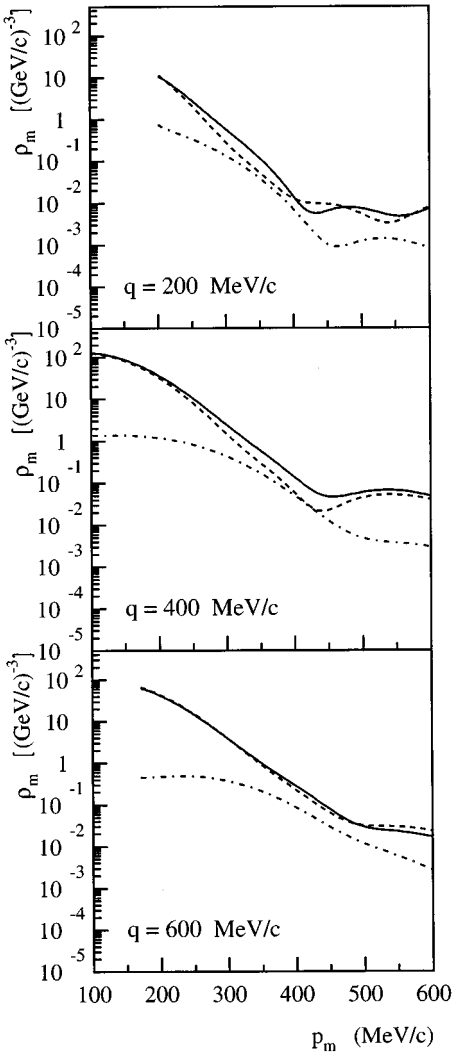

FIG. 2. Reduced cross section for proton knockout from the $1p_{3/2}$ shell in ^{16}O for $\epsilon = 500$ MeV, $\omega = 100$ MeV, and different values of the momentum transfer. The dashed and dash-dotted lines give the one-body and two-body (mesonic) contributions, respectively, to the reduced cross section. The solid line is the coherent sum of these two contributions. The curves are not multiplied by a spectroscopic factor.

tion. *Second*, the kinematics considered in Figs. 1 and 2 are such that the energy transfer and the energy of the incoming electron are fixed. This means that the higher the momentum transfer, the more important the transverse part of the cross section will be. As mesonic currents contribute only to the transverse components of the cross section and do not affect the longitudinal part, we can conclude that mesonic currents gain in relative importance with increasing q.

Summarizing, we conclude that the considered ^{16}O$(e,e'p)$ cross section is strongly affected by the FSI and mesonic currents even for relatively large-q values. Accordingly, this could seriously hamper the extraction of any information on the single-particle spectral function. A naive suggestion would be to study the high-momentum side of the cross section for higher-energy transfer since the FSI vanishes for $p_p \to \infty$. On the contrary, for these higher-energy transfers it is to be expected that isobaric currents gain in importance.

IV. RESULTS FOR ^{208}Pb$(e,e'p)$

In Figs. 4–6 we plot the reduced cross section for proton knockout from the $3s_{1/2}$ and $2d_{3/2}$ shells in ^{208}Pb. The kinematics coincide with the experimental conditions from Ref. [7].

It goes without saying that the large number of protons and neutrons makes the ^{208}Pb$(e,e'p)$ calculations rather complicated when accounting for two-body photoabsorption mechanisms. Moreover, for a nucleus containing 82 protons electron distortion effects can no longer be neglected.

Let us first assume a direct knockout mechanism. In such a picture, the proton is ejected from the nucleus in a one-step reaction mechanism after photoabsorption on the one-body

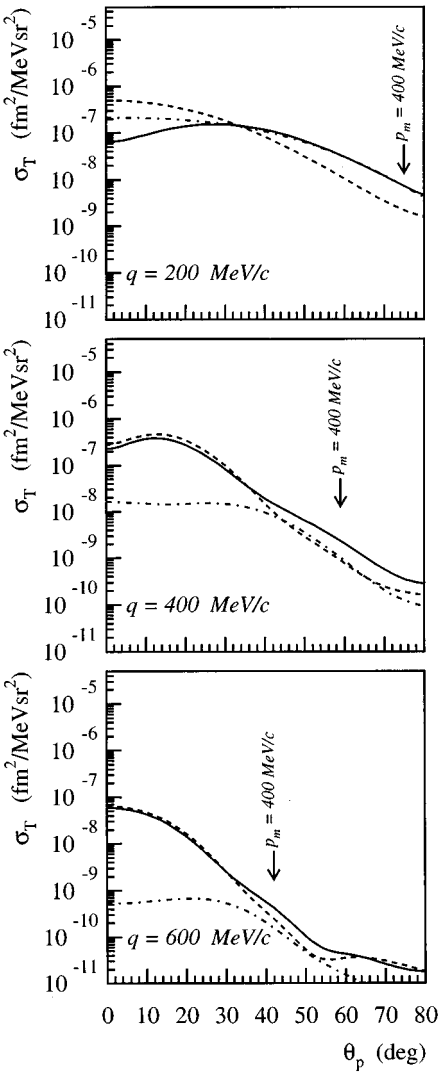

FIG. 3. Transverse cross section σ_T for the ^{16}O$(e,e'p)$ reaction for the same kinematics as in Fig. 2. We adopt the line conventions as defined in Fig. 2. The curves are not multiplied by a spectroscopic factor.

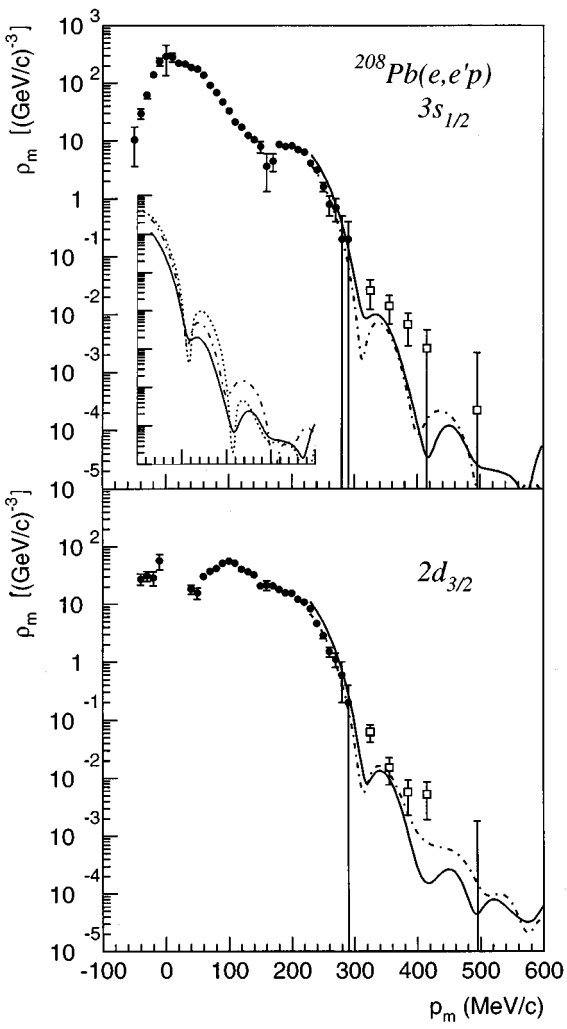

FIG. 4. ^{208}Pb$(e,e'p)$ reduced cross sections for the kinematics of the experiments by Bobeldijk *et al.* [7]. For the dash-dotted lines the FSI is treated in the HF approach, whereas for the solid line the optical potential model is adopted. The optical potential calculations are multiplied by the spectroscopic factors $[S(3s_{1/2})=0.51, S(2d_{3/2})=0.54]$. The HF curves are multiplied by $S=0.15$ for both states. The data are taken from Refs. [7] (squares) and [26] (dots). In the inset we compare the PWIA (dotted line), the HF, and the optical potential results. In this case the three curves are not scaled by a spectroscopic factor.

nuclear current. The results are plotted in Fig. 4. The FSI is handled within two different approaches: the HF approach and the optical potential model (OPM). In both approaches the bound-state wave functions are evaluated with the HF mean-field potential. Whereas in the HF approach the continuum single-particle states are derived from the same real HF potential, in the optical potential calculation the scattering potential is a combination of a real and an imaginary potential constructed from the general parametrization of elastic proton scattering data by Schwandt *et al.* [27]. Both models for the FSI yield very similar quantitative results for the reduced cross section. However, we have to keep in mind that a considerably smaller reduction factor $[S(3s_{1/2})=0.15, S(2d_{3/2})=0.15]$ is adopted for the HF result compared to the spectroscopic factor $[S(3s_{1/2})=0.51, S(2d_{3/2})=0.54]$ used for the optical potential calculation. This large difference can best be illustrated by the inset in Fig. 4. The optical potential calculation causes a quenching of the PWIA $(e,e'p)$ strength at the maxima of the reduced cross section. In addition, one observes considerably less pronounced minima. It is obvious that due to the lack of an absorptive imaginary potential, the HF approach is not able to reproduce this strong quenching effect but predicts a similar shape of the reduced cross section as derived with the OPM. In the HF approach, the transparency, i.e., the probability that the struck proton emerges from the nucleus without a collision with the other nucleons in the nucleus, is considered to be one. However, experimental predictions for the transparency of a nucleus extracted from $(e,e'p)$ experiments vary from 0.8 to 0.4 for target nuclei in the range $A=12$–181 [28,29]. These numbers can be reproduced within the model of Pandharipande and Pieper [30] by adopting the correlated Glauber approximation and accounting for a density dependence of the nucleon-nucleon interaction. This means that for heavy target nuclei the absorptive part of the optical potential causes a strong reduction of the cross

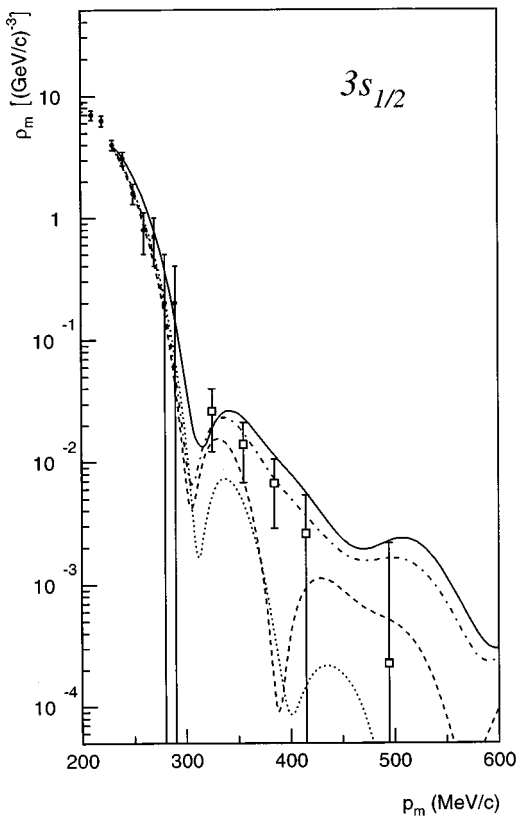

FIG. 5. Systematic study of the high-momentum components in the ^{208}Pb$(e,e'p)$ cross section for proton knockout from the $3s_{1/2}$ shell ($\epsilon=487$ MeV, $q=221$ MeV/c, and $\omega=110$ MeV). The data are taken from Refs. [7] (squares) and [26] (dots). The dotted curve represents the results from the HF calculation. The dashed, dash-dotted, and solid lines result from, respectively, the RPA, the RPA +two-body nuclear currents, and the RPA+two-body nuclear currents+Coulomb distortion calculation. All the curves are multiplied by $S=0.15$.

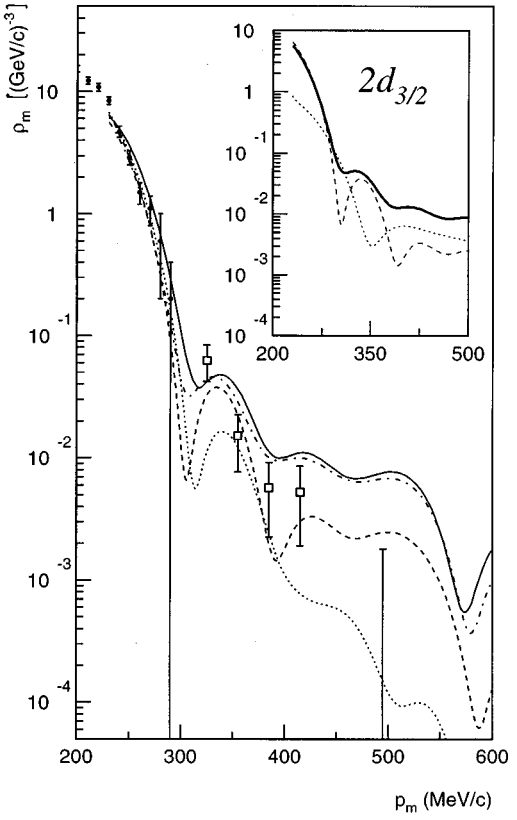

FIG. 6. Same as Fig. 5, but for proton knockout from the $2d_{3/2}$ shell. In the inset we plot the one-body (dashed line) and two-body (dotted line) current contributions to the reduced ^{208}Pb$(e,e'p)$ cross section. The solid line is the coherent sum of the two curves.

section by a factor 2.5, in this way explaining the small spectroscopic factor extracted within our HF approach. On the other hand, for light nuclei, the OPM and the HF approach are expected to produce spectroscopic factors that do not differ by more than 20%. The ^{16}O$(e,e'p)$ analysis reported in Ref. [19] seems to confirm this observation.

An important advantage of the HF approach is the fact that both bound and continuum single-particle states are derived from the same real mean-field potential, respecting in this way orthogonality between the continuum and bound states. It is well known that any deviation of this orthogonality requirement might cause substantial spurious contributions to enter the $(e,e'p)$ cross sections and that this problem is predominantly manifest at high p_m [31]. In order to avoid these complications, we consider the HF-RPA approach as a good starting point to study the relative importance of higher-order mechanisms in the quasielastic $(e,e'p)$ reaction.

From Fig. 4 it is clear that the adopted direct knockout picture underestimates the measured $(e,e'p)$ strength at high missing momenta ($p_m>300$ MeV/c). In conformity with the results for the ^{16}O$(e,e'p)$ reaction, we expect that multistep processes of the RPA type, photoabsorption on two-body nuclear currents, and Coulomb distortion effects will modify the reduced cross sections. The following discussion is meant to find out the *relative* importance of these higher-order effects to the $(e,e'p)$ cross section.

In going from the HF approach with only one-body components in the nuclear current to a more complete calculation that includes long-range correlations of the RPA type, two-body nuclear currents, and electron distortion effects (Figs. 5 and 6), an enhancement of strength, especially in the high-momentum tail of the cross section, is observed. The ^{208}Pb$(e,e'p)$ experiment was done in the high-energy tail of the quasielastic peak. Therefore, it is not surprising that processes beyond the direct knockout picture come into play. All the curves in Figs. 5 and 6 are multiplied by the same scaling factor ($S=0.15$).

The role of RPA correlations is mainly manifest at the high-momentum side of the reduced cross section. A possible explanation is the following. Multistep processes tend to redistribute the strength over a wider missing momentum range and, consequently, shift some strength from the lower to the higher p_m region [32]. Indeed, after a number of rescattering processes the detected kinetic energy of the escaping nucleon no longer uniquely determines the momentum of the nucleon on which the initial photoabsorption took place. Combining both considerations, the reduced cross section

does not scale as a function of the missing momentum when RPA correlations are accounted for and the $(e,e'p)$ strength is smeared out towards higher missing momenta.

In a similar way one can explain the substantial contribution of two-body nuclear currents to the reduced cross section. Electroinduced one-proton knockout after photoabsorption on a two-body nuclear current also generates a considerable amount of strength at the high missing momentum side of the reduced cross section. As demonstrated in the inset of Fig. 6, a coherent sum of the one-body and two-body nuclear current contributions is required. The pure two-body contribution shows a much smoother behavior as a function of p_m compared to the one-body part. This can be easily explained from the fact that for the two-body absorption mechanism the missing momentum p_m no longer serves as a scaling variable. Moreover, whereas for the low missing momentum side the strength generated by the two-body mesonic currents is at least an order of magnitude smaller than the pure nucleonic contribution (which is equal to the one-body nuclear current), for the highest missing momenta the two-body strength *can* overshoot the one-body contribution. Consequently, the reduced cross section at the low missing momentum side can be mainly attributed to proton knockout after photoabsorption on a one-body nuclear current. To the contrary, two-body current contributions and interference effects between the one- and two-body parts in the nuclear current come into play for the high missing momentum side of the reduced cross section.

In the paper by Bobeldijk *et al.* [7] the effect of mesonic currents is estimated at 10% of the one-body contribution. This number is based on a calculation for ^{40}Ca [33]. However, as demonstrated for the target nuclei ^{16}O (Fig. 2) and ^{208}Pb (Figs. 5 and 6), the relative contribution of two-body nuclear currents to the reduced cross section exhibits a clear mass dependence. At high missing momenta, mesonic currents seem to be relatively more important for the ^{208}Pb$(e,e'p)$ compared to the ^{16}O$(e,e'p)$ cross sections when considering comparable kinematic conditions. This observation is not too surprising. In contrast with the particle-hole matrix element for the one-body current, the matrix elements for the two-body currents involve a summation over the different occupied states in the target nucleus [19]. In this way, a clear mass dependence is introduced in the two-body current contribution.

Considering the $(e,e'p)$ reaction from a heavy nucleus such as ^{208}Pb, Coulomb distortion effects cannot be discarded. It is clearly seen from Figs. 5 and 6 that electron distortion effects modify the shape of the reduced cross sections for proton knockout from the two shells considered. The size of the corrections related to Coulomb distortion depends on the quantum numbers of the shell from which the proton is ejected. We notice that the $3s_{1/2}$ reduced cross section is affected more by electron distortion effects than the $2d_{3/2}$ result. For the two single-particle states, the Coulomb distortions induce strength at high missing momenta and fill up the minima of the reduced cross sections.

We may conclude that all three higher-order effects taken into consideration in our study improve on the agreement with the data as they account for part of the missing $(e,e'p)$ strength at high missing momenta. In a recent paper by Bobeldijk *et al.* [7] the ^{208}Pb $(e,e'p)$ data at high missing momenta were analyzed within the framework of the Coulomb distorted-wave impulse approximation (CDWIA) approach of Boffi *et al.* [2]. The bound-state Wood-Saxon wave functions adopted in this model were modified with various types of correlation functions. These correlation functions account in a semiphenomenological way for short-range and long-range nucleon-nucleon correlations that are not implemented in the mean-field single-particle wave functions. In conformity with the predictions of Müther and Dickhoff [8], Bobeldijk *et al.* arrived at a small effect of the SRC at the low missing energies probed in the experiment. They attributed the mismatch between the CDWIA (no correlation functions included) approach and the data to long-range effects in the nuclear wave function. These results partially agree with our results. Indeed, as can be learned from our calculations, long-range correlations (of the RPA type) considerably contribute to the cross section at high missing momenta. In our model, however, the calculated mesonic contribution to the reduced cross section is found to be considerably larger than the estimation reported in the paper by Bobeldijk *et al.*

Recently, also a fully relativistic analysis of the ^{208}Pb$(e,e'p)$ results at high p_m has become available [34]. In comparison to the nonrelativistic approaches, the relativistic models reduce the quasielastic $(e,e'p)$ cross section at low missing momenta [24,34]. At high missing momenta the opposite behavior is noticed. The degree to which these effects occur is, however, strongly dependent on the adopted choice for the relativistic off-shell nuclear current operator. The relativistic calculations of Ref. [34] made it clear that the predicted sensitivity to the choice of the current operator is more pronounced at high p_m than at low p_m. In that sense, the conclusions are similar to those drawn within our nonrelativistic treatment. The off-shell behavior of the relativistic nuclear current operator could indeed be considered as an effective way of accounting for the many-body correlations (such as ground-state correlations and meson-exchange currents) in the $(e,e'p)$ reaction process. In that respect it is worth mentioning that the qualitative effect of the RPA ground-state correlations on the $(e,e'p)$ cross sections of Figs. 5 and 6 is similar to the effect being ascribed to relativity in Ref. [34]: a (modest) decrease of the strength at low p_m and a considerable increase at high p_m.

V. CONCLUSIONS

In this paper we have reported on the $(e,e'p)$ reaction at high missing momenta and low missing energies. We confronted our ^{208}Pb results with data taken by Bobeldijk *et al.* This experiment was primarily meant to investigate the short-range nucleon-nucleon correlations in the nucleus as they are known to show up at high momenta in the nucleon momentum distribution. Starting from the direct knockout picture for one-proton knockout reactions, our model implements higher-order effects such as correlations of the RPA type, photoabsorption on two-body one-pion exchange currents, and electron distortion effects in a systematic and consistent way. It has been shown that all these effects strongly modify the reduced cross section at high missing momenta. Notwithstanding the fact that the direct knockout picture is

sufficient to reproduce the low missing momentum side of the reduced cross section, these higher-order effects need to be carefully examined before any conclusions on the role of nucleon-nucleon correlations for the high-momentum components in the nucleon momentum distribution can be drawn from $(e,e'p)$ data.

ACKNOWLEDGMENTS

The authors are grateful to K. Heyde for fruitful discussions and suggestions. This work has been supported by the Inter-University Institute for Nuclear Sciences (IIKW) and the National Fund for Scientific Research (NFWO).

[1] S. Frullani and J. Mougey, Adv. Nucl. Phys. **14**, 1 (1984).
[2] S. Boffi, C. Giusti, and F.D. Pacati, Phys. Rep. **226**, 1 (1993).
[3] J.J. Kelly, Adv. Nucl. Phys. **23**, 75 (1996).
[4] O. Benhar and V.R. Pandharipande, Rev. Mod. Phys. **65**, 817 (1993).
[5] C. Mahaux and R. Sartor, Adv. Nucl. Phys. **20**, 1 (1991).
[6] K.I. Blomqvist *et al.*, Phys. Lett. B **344**, 85 (1995).
[7] I. Bobeldijk *et al.*, Phys. Rev. Lett. **73**, 2684 (1994).
[8] H. Müther and W.H. Dickhoff, Phys. Rev. C **49**, R17 (1994).
[9] A. Polls, H. Müther, and W.H. Dickhoff, Nucl. Phys. **A594**, 117 (1995).
[10] H. Müther, A. Polls, and W.H. Dickhoff, Phys. Rev. C **51**, 3040 (1995).
[11] O. Benhar, A. Fabrocini, S. Fantoni, and I. Sick, Nucl. Phys. **A579**, 493 (1994).
[12] D. Van Neck, A.E.L. Dieperink, and E. Moya de Guerra, Phys. Rev. C **51**, 1800 (1995).
[13] A.N. Antonov, M.V. Stoitsov, M.K. Gaidarov, S.S. Dimitrova, and P.E. Hodgson, J. Phys. G **21**, 1333 (1995).
[14] M.K. Gaidarov, A.N. Antonov, G.S. Anagnostatos, S.E. Massen, M.V. Stoitsov, and P.E. Hodgson, Phys. Rev. C **52**, 3026 (1995).
[15] A.S. Raskin and T.W. Donnelly, Ann. Phys. (N.Y.) **191**, 78 (1989).
[16] J. Ryckebusch, M. Waroquier, K. Heyde, J. Moreau, and D. Ryckbosch, Nucl. Phys. **A476**, 237 (1988).
[17] M. Waroquier, J. Ryckebusch, J. Moreau, K. Heyde, N. Blasi, S.Y. van der Werf, and G. Wenes, Phys. Rep. **148**, 249 (1987).
[18] D.O. Riska, Phys. Rep. **181**, 207 (1989).
[19] V. Van der Sluys, J. Ryckebusch, and M. Waroquier, Phys. Rev. C **49**, 2695 (1994).
[20] H. Überall, *Electron Scattering from Complex Nuclei* (Academic, London, 1971).
[21] V. Van der Sluys, J. Ryckebusch, and M. Waroquier (in preparation).
[22] Y. Jin, D.S. Onley, and L.E. Wright, Phys. Rev. C **45**, 1311 (1992).
[23] Y. Jin, D.S. Onley, and L.W. Wright, Phys. Rev. C **50**, 168 (1994).
[24] J.M. Udias, P. Sarriguren, E. Moya de Guerra, E. Garrido, and J.A. Caballero, Phys. Rev. C **48**, 2731 (1993).
[25] T.D. DeForest, Jr., Nucl. Phys. **A392**, 232 (1983).
[26] E.N.M. Quint, Ph.D. thesis, University of Amsterdam, 1988.
[27] P. Schwandt *et al.*, Phys. Rev. C **26**, 55 (1982).
[28] G. Garino *et al.*, Phys. Rev. C **45**, 780 (1992).
[29] D.F. Geesaman *et al.*, Phys. Rev. Lett. **63**, 734 (1989).
[30] V.R. Pandharipande and S.C. Pieper, Phys. Rev. C **45**, 791 (1992).
[31] S. Boffi, R. Cenni, C. Giusti, and F.D. Pacati, Nucl. Phys. **A420**, 38 (1984).
[32] J.J. Kelly, in *Proceedings of the Second Workshop on Electromagnetically Induced Two-nucleon Emission, Gent, 1995,* edited by J. Ryckebusch and M. Waroquier (UE Press, Gent, 1995), pp. 269–274.
[33] S. Boffi and M. Radici, Phys. Lett. B **242**, 151 (1990).
[34] J.M. Udías, P. Sarriguren, E. Moya de Guerra, and J.A. Caballero, Phys. Rev. C **53**, R1488 (1996).